Mesozoic 001 (2): 159–172
https://www.mapress.com/mz/

Article

ISSN 3021-1859 (print edition)
MESOZOIC
ISSN 3021-1867 (online edition)

https://doi.org/10.11646/mesozoic.1.2.8
http://zoobank.org/urn:lsid:zoobank.org:pub:9BEC04AE-88A8-41F8-BD0D-067F993B6D58

Newly identified late Early Cretaceous volcanic rocks in the Beixiangshan area, Lower Yangtze River Belt, South China and its implications

HAI-LONG GAO[1], YONG ZHANG[2,*], YI-TONG SU[2], LIN-WEI SHEN[1], HUAN-YU LIAO[3], XIAO-MEI NIE[4] & DI-YING HUANG[2,*]

[1]*School of Earth Sciences, East China University of Technology, Nanchang, Jiangxi 330013, China*
[2]*State Key Laboratory of Palaeobiology and Stratigraphy, Nanjing Institute of Geology and Palaeontology, Chinese Academy of Sciences, Nanjing 210008, China*
[3]*Institute of Palaeontology, Yunnan Key Laboratory of Earth System Science, Yunnan Key Laboratory for Palaeobiology, MEC International Joint Laboratory for Palaeobiology and Palaeoenvironment, Yunnan University, Kunming 650500, China*
[4]*School of Earth Sciences, School of Marine Science and Technology, China University of Geosciences, Wuhan 430074, China*
cugloong@163.com; https://orcid.org/0000-0002-6365-9983
yzhang@nigpas.ac.cn; https://orcid.org/0000-0001-8237-6498
ytsu@nigpas.ac.cn; https://orcid.org/0000-0003-0547-0792
1042203791@qq.com; https://orcid.org/0009-0003-8355-004X
hyliao@ynu.edu.cn; https://orcid.org/0000-0002-3004-056X
xiaomeinie2013@126.com; https://orcid.org/0000-0002-8825-6048
dyhuang@nigpas.ac.cn; https://orcid.org/0000-0002-5637-4867
**Corresponding authors*

Abstract

The magmatic events in the Lower Yangtze River Belt could be divided into four stages: 148–133 Ma, 131–127 Ma, 127–121 Ma, and 109–100 Ma. The final episode is represented by the intrusions in the Ningzhen area, however no contemporaneous volcanic rocks have been reported. In this study, we present an integrated analysis of petrology, zircon U-Pb ages, and whole rock major-trace elements for newly identified volcanic rocks in the Beixiangshan area. Zircon U-Pb dating yields an eruption age of 106.3 ± 0.4 Ma, indicating that these rocks likely belong to the lower part of the Pukou Formation. The volcanic rocks exhibit arc-like geochemical features, distinct from those of the intrusions in the Ningzhen area. The volcanic rocks may be formed during a tectonic transition phase from compression to extension, due to the direction changes of plate convergence. The widespread angular unconformity around the volcanic rocks may represent episode C of the Yanshanian tectonic event, based on the dating work on volcanic rocks, its minimum age should be *ca*. 106 Ma.

Keywords: Early Cretaceous, Lower Yangtze River Belt, Yanshanian, magmatism, Ningzhen

Introduction

The Lower Yangtze River Belt (LYRB) is the most important Cu-Fe-Au-Mo polymetallic metallogenic belt in China, and these deposits are genetically related to Cretaceous igneous rocks (*e.g.*, Ling *et al*., 2009; Yan *et al*., 2021). Therefore, extensive research has been carried out on the petrogenesis, magmatism, tectonics, and mineralization in this region (*e.g.*, Tang *et al*., 2013; Chen *et al*., 2014, 2016; Wang F. *et al*., 2014; Zhou *et al*., 2015; Sun *et al*., 2021).

Based on published geochronological data (*e.g.*, Liu *et al*., 2014; Xue, 2019), the Cretaceous magmatism and mineralization in the LYRB could be divided into four stages: 148–133 Ma, 131–127 Ma, 127–121 Ma and 109–101 Ma, showing an eastward younging trend (Wang F. *et al*., 2014; Yan *et al*., 2015). The last episode of magmatic activity was typical in the intermediate-acid intrusions in the Ningzhen area, such as Anjishan, Gaozi, Xinqiao, and Shima plutons (Zeng *et al*., 2013; Liu *et al*., 2014; Xue, 2019). The ages and geochemical characteristics of these intrusions were well constrained, while volcanic rocks from the same period have not yet been reported.

In this paper, we present an investigation on the petrology, zircon U-Pb ages, and whole rock geochemistry for a suit of newly identified volcanic rocks at the summit of the Beixiangshan, Nanjing, Jiangsu Province (Fig. 1). The aims are to: 1) constrain their eruption ages and geochemical characteristics; 2) elucidate their petrogenesis and tectonic environment; and 3) conduct

Submitted: 23 May 2024; accepted by Z. Feng: 21 Jun. 2024; published: 27 Jun. 2024

regional stratigraphic correlation and provide insights into their tectonic implications.

Geological setting

The LYRB is located on the northeastern part of the South China Block, separated by the Xiangfan-Guangji and the Tan-Lu faults from the Dabie orogenic belt to the west, and bounded by the Yangxing-Changzhou Fault to the south (Fig. 1B, Sun *et al*., 2017). The South China Block consists of the Yangtze Block in the west and the Cathaysia Block in the east, and they collided along the Jiangshan-Shaoxing suture during the early Neoproterozoic period (~1.1–0.9 Ga, Chen *et al*., 1991; Li *et al*., 2014b). As an ultrahigh-pressure metamorphic belt, the Qinling-Dabie orogenic belt formed from the collision between the North and South China blocks in the Late Triassic (Meng & Zhang, 1999). The Paleo-Pacific plate began to subduct beneath the eastern Eurasian continent since the Late Triassic or Early Jurassic (Guo *et al*., 2015; Xu *et al*., 2017). The Triassic and Jurassic-Cretaceous tectonothermal events were also referred to as Indosinian and Yanshanian movements, respectively, in some Chinese literature (Wong, 1927; Zhao, 1990; Wang *et al*., 2013). The NE- to NNE-striking Tan-Lu Fault is a giant fault parallel to the subduction zone of Paleo-Pacific, making it a valuable indicator for revealing subduction history in the western Pacific region (Zhu *et al*., 2018). The Tan-Lu fault originated during the collision of North China and South China blocks and reactivated several times in response to oceanic plate subduction in the western Pacific region (Zhu *et al*., 2018).

The intrusions are widely distributed in the LYRB while the volcanic rocks are mainly found in the pull-

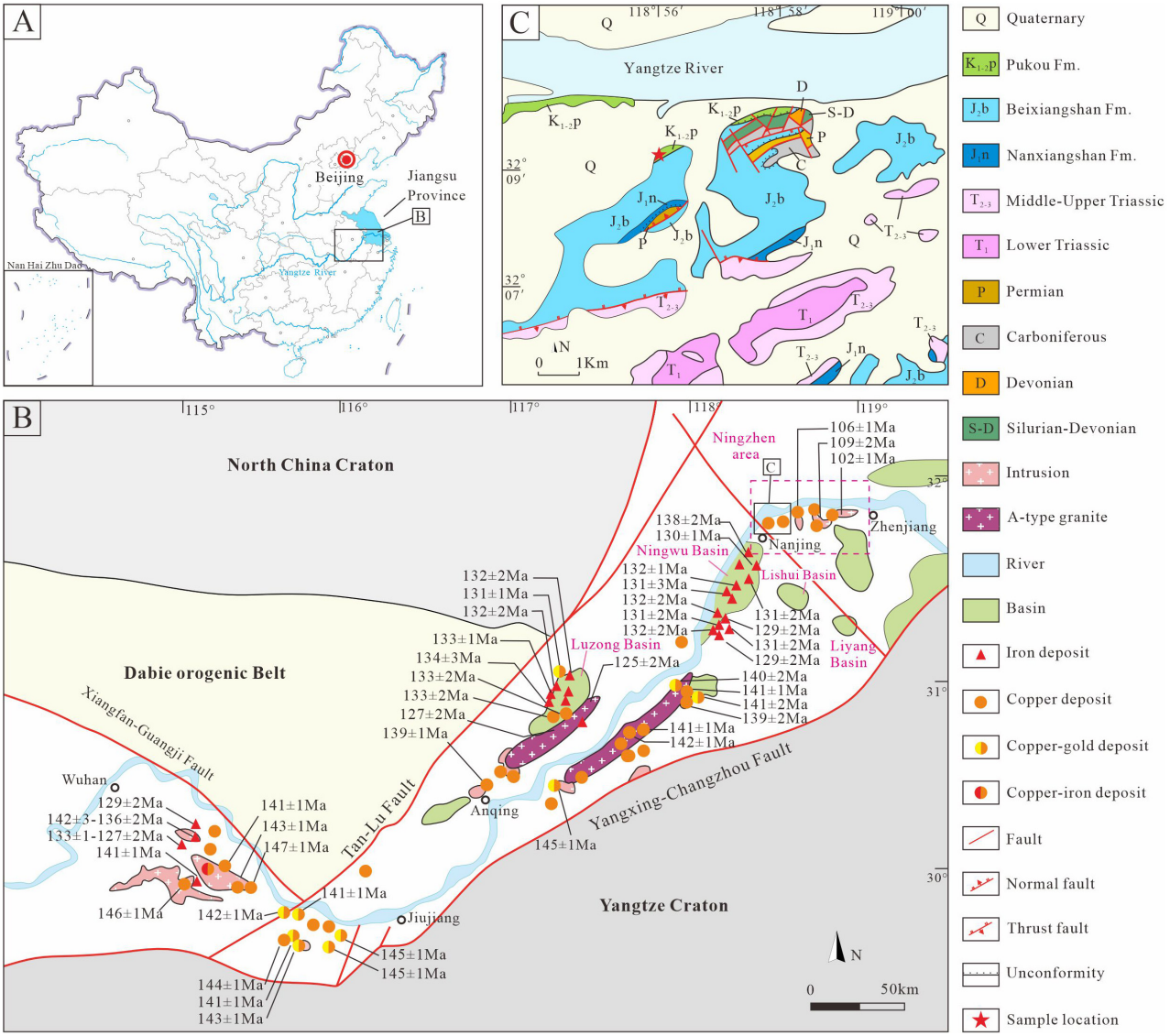

FIGURE 1. Locality maps. **A**, The geographic location of the LYRB. **B**, The simplified tectonic map, modified after Sun *et al*., 2017. **C**, The simplified geological map of the study area. The chronological data are from Sun *et al*., 2017 and reference therein.

apart basins (Chen *et al*., 2016; Sun *et al*., 2017), such as Luzong, Ningwu, Lishui, and Liyang basins (Fig. 1B; Mao *et al*., 2011; Sun *et al*., 2017).

The volcanic rocks within the Ningwu Basin can be subdivided into four units, known as the Longwangshan, Dawangshan, Gushan, and Niangniangshan formations in ascending order (Chen *et al*., 2016). They consist mainly of trachyandesite, andesite, trachyte, dacite, breccia, and tuff, with minor alkaline basalt, basaltic andesite, rhyolite, and phonolite (Tang *et al*., 2013). Most of the volcanic rocks are high-K calc-alkaline to calc-alkaline series, with the majority exhibiting adakitic geochemical signatures (Zhou *et al*., 2015), and their ages vary within a relatively short period, *i.e.* 135–126 Ma (*e.g*., Zhou *et al.*, 2011; Tang *et al*., 2013; Chen *et al*., 2016).

Several intrusions with a dating of 109–101 Ma have been exposed in the Ningzhen area (Fig. 1B), and they represent the youngest known Mesozoic magmatism (Zeng *et al*., 2013; Liu *et al*., 2014; Xue, 2019; Sun *et al*., 2021) in the LYRB. In contrast, no contemporaneous volcanic rocks have been reported. The uppermost layer in this region containing volcanic rocks is the Lower-Upper Cretaceous Pukou Formation (Fig. 1C). The Pukou Formation could be subdivided into four members (Yan *et al*., 2001). Member 1 consists of conglomerate, andesite, volcanic breccia and sandstone, without fossils (JBGMR, 1997; Yan *et al*., 2001). Members 2 and 3 consist of brown mudstone and siltstone with interlayered salt rocks (Yan *et al*., 2001). Sporopollen, such as *Schizaeoisporites, Welwitschiapites, Classopolli*s, and *Ephedripites* (Song, 1986; Yan *et al.*, 2001), have been identified in the mudstone. Member 4 is composed of brown mudstone, silt-mudstone and layered grey siltstone. Except for the sporopollen, the ostracod (*Tangxiella—Talicypridea—Cypridea*) and the charophyte (*Euaclistochara mundula—Maedlerisphaera corollacea*) were also discovered in this part (Yan *et al*., 2001 and reference therein). Based on the *Schizaeoisporites—Classopollis* sporopollen assemblage and the appearance of *oblate tricolporate* and *triporate* pollen grains, the Pukou Formation was constrained to be late Albian to Cenomanian period (Song, 1986; Yan *et al*., 2001).

Material and methods

Sampling

The exposed sedimentary strata in the Beixiangshan area include the Middle Permian Gufeng Formation, the Lower to Middle Jurassic Nanxiangshan Formation, and the Middle Jurassic Beixiangshan Formation (Fig. 2). At the summit of the mountain, a suit of intermediate volcanic rocks, previously considered as the Jurassic Longwangshan Formation or the upper part of the Jurassic Xiangshan Group (Ju, 1987; GBAP, 1986; JBGMR, 1997), overlies the sediments with an angular unconformity, indicating a sedimentary hiatus over an extended period. The Xiangshan Group was divided into the Nanxiangshan and Beixiangshan formations in ascending order (Ju, 1987). The Lower Jurassic Nanxiangshan Formation is characterized by coal-bearing strata, containing abundant plant and bivalve fossils (JBGMR, 1997). The overlaying Beixiangshan Formation is a series of clastic and volcanoclastic rocks, which have been assigned to be Middle Jurassic due to the sporopollen fossils (Huang, 2000). The Longwangshan Formation consists of andesitic volcanic breccia, sedimentary volcanic breccia, lava, and intercalated tuffaceous siltstone (Zhou *et al.*, 2011). This unit overlies the Beixiangshan Formation with a disconformity. The volcanic rocks from the Longwangshan Formation yielded zircon U-Pb ages of 133–131 Ma (Zhang *et al.*, 2003; Zhou *et al.*, 2011; Tang *et al.*, 2013).

The volcanic rocks are purple in colour, and primarily consist of andesite and andesitic breccia (Fig. 2A, B). One sample (BXS21z) was collected for the zircon U-Pb dating, and six samples (listed in Table 2) were designated for whole rock major-trace elements analyses. The rocks are primarily comprised of plagioclase (60–70 vol.%), lithic fragments (10–20 vol.%), biotite (~ 10 vol.%), iron oxide (~ 5 vol.%) with a minor quartz content (< 5 vol.%) (Figs 2 C–F). A lot of grains exceed 2 mm in size, thus the sample BXS21z is designated as volcanic breccia.

Methods

The zircon grains were separated by conventional magnetic and heavy liquid techniques and hand-picking under a binocular microscope. The selected zircon grains were then mounted in epoxy resin, polished and gold-coated for analysis. Photographs of the grains were captured under transmitted and reflected light, in addition to cathodoluminescence (CL) imaging (Fig. 3), to facilitate the identification of suitable spots for in situ analysis. The zircon U-Pb isotopic analyses were conducted using an Agilent 7500 LA-ICP-MS instrument at the State Key Laboratory of Continental Dynamics, Northwest University, Xi'an, China. The off-line selection and integration of background and signals, time-drift correction and quantitative calibration were conducted using GLITTER 4.0 software. Zircon U-Pb concordia and weighted mean age plots were produced using Isoplot/Ex_ver3.0 (Ludwig, 2003). The analytical results are presented in Table 1.

Six samples were sectioned into slices, followed by

TABLE 1. Results of LA-ICP-MS zircon U-Pb analyses for volcanic rocks from Beixiangshan, Nanjing, Lower Yangtze River Belt.

Analyses					$^{207}Pb/^{206}Pb$		$^{207}Pb/^{235}U$		$^{206}Pb/^{238}U$		$^{207}Pb/^{206}Pb$		$^{207}Pb/^{235}U$		$^{206}Pb/^{238}U$		
	Pb	Th	U	Th/U	Ratio	1σ	Ratio	1σ	Ratio	1σ	Age	1σ	Age	1σ	Age	1σ	concordance
BXS021-01	6.5	385.0	251.6	1.5	0.04817	0.00229	0.11097	0.00508	0.0167	0.00019	107.6	108.5	106.8	1.2	106.9	1.2	99.9
BXS021-02	5.9	355.8	225.2	1.6	0.04845	0.0026	0.11223	0.00583	0.01679	0.00021	121.5	121.8	107.4	1.3	108	1.3	99.4
BXS021-03	12.1	639.2	483.6	1.3	0.04919	0.00213	0.11278	0.00469	0.01663	0.00018	156.7	98.4	106.3	1.1	108.5	1.1	98.0
BXS021-05	7.4	471.4	312.5	1.5	0.04889	0.00285	0.10512	0.00595	0.01559	0.0002	142.4	131.6	99.7	1.3	101.5	1.3	98.2
BXS021-06	8.2	583.5	306.8	1.9	0.04921	0.00226	0.11265	0.00499	0.0166	0.00018	158	104.2	106.1	1.1	108.4	1.1	97.9
BXS021-08	10.7	875.8	364.5	2.4	0.04997	0.00234	0.11109	0.005	0.01612	0.00018	193.7	105.2	103.1	1.1	107	1.1	96.4
BXS021-09	9.4	662.6	330.5	2.0	0.0504	0.0027	0.11697	0.00607	0.01683	0.00021	213.4	119.8	107.6	1.3	112.3	1.3	95.8
BXS021-10	14.5	1104.5	506.3	2.2	0.04991	0.0021	0.11279	0.00455	0.01639	0.00017	190.7	95.1	104.8	1.1	108.5	1.1	96.6
BXS021-11	7.8	456.0	298.7	1.5	0.05098	0.00277	0.11705	0.00614	0.01665	0.00022	239.9	120.6	106.5	1.4	112.4	1.4	94.8
BXS021-12	6.4	362.2	251.5	1.4	0.04865	0.00253	0.11223	0.00564	0.01673	0.00019	130.9	117.7	107	1.2	108	1.2	99.1
BXS021-14	10.1	787.7	395.2	2.0	0.0473	0.00197	0.10055	0.00402	0.01542	0.00015	63.7	96.8	98.6	0.9	97.3	0.9	98.7
BXS021-15	4.1	144.6	149.6	1.0	0.05151	0.00453	0.14253	0.01221	0.02007	0.0004	263.9	190.0	128.1	2.5	135.3	2.5	94.7
BXS021-17	8.5	483.4	326.0	1.5	0.04841	0.0024	0.11341	0.00543	0.01699	0.0002	119.3	113.0	108.6	1.3	109.1	1.3	99.5
BXS021-18	29.9	515.2	661.2	0.8	0.05163	0.00156	0.24774	0.00701	0.0348	0.00029	269.1	67.7	220.5	1.8	224.7	1.8	98.1
BXS021-19	17.1	328.5	544.3	0.6	0.05016	0.00168	0.17236	0.00547	0.02492	0.00022	202.4	76.1	158.7	1.4	161.5	1.4	98.3
BXS021-21	5.8	326.1	219.6	1.5	0.04873	0.00279	0.11549	0.00642	0.01719	0.00021	134.8	129.3	109.9	1.3	111	1.3	99.0
BXS021-24	8.3	679.3	310.3	2.2	0.04958	0.00327	0.11115	0.00712	0.01626	0.00025	175.2	147.1	104	1.6	107	1.6	97.2
BXS021-25	8.3	599.9	295.6	2.0	0.04962	0.00231	0.11636	0.00523	0.01701	0.00018	177.2	105.3	108.7	1.2	111.8	1.2	97.2
BXS021-26	4.4	264.4	178.7	1.5	0.04925	0.00303	0.11159	0.00666	0.01643	0.00022	159.6	137.8	105.1	1.4	107.4	1.4	97.9
BXS021-27	5.0	306.5	196.9	1.6	0.04939	0.00397	0.11282	0.00882	0.01657	0.0003	166.2	177.6	105.9	1.9	108.5	1.9	97.6
BXS021-29	5.2	258.8	223.4	1.2	0.04977	0.00355	0.11365	0.00788	0.01656	0.00027	184.5	158.3	105.9	1.7	109.3	1.7	96.9
BXS021-31	9.9	724.9	367.1	2.0	0.04729	0.0021	0.10841	0.00463	0.01662	0.00017	63.4	102.8	106.3	1.1	104.5	1.1	98.3

Analyzers are Agilent 7500, the laser is 32μm and the error is 1 σ. Calculated by Glitter.

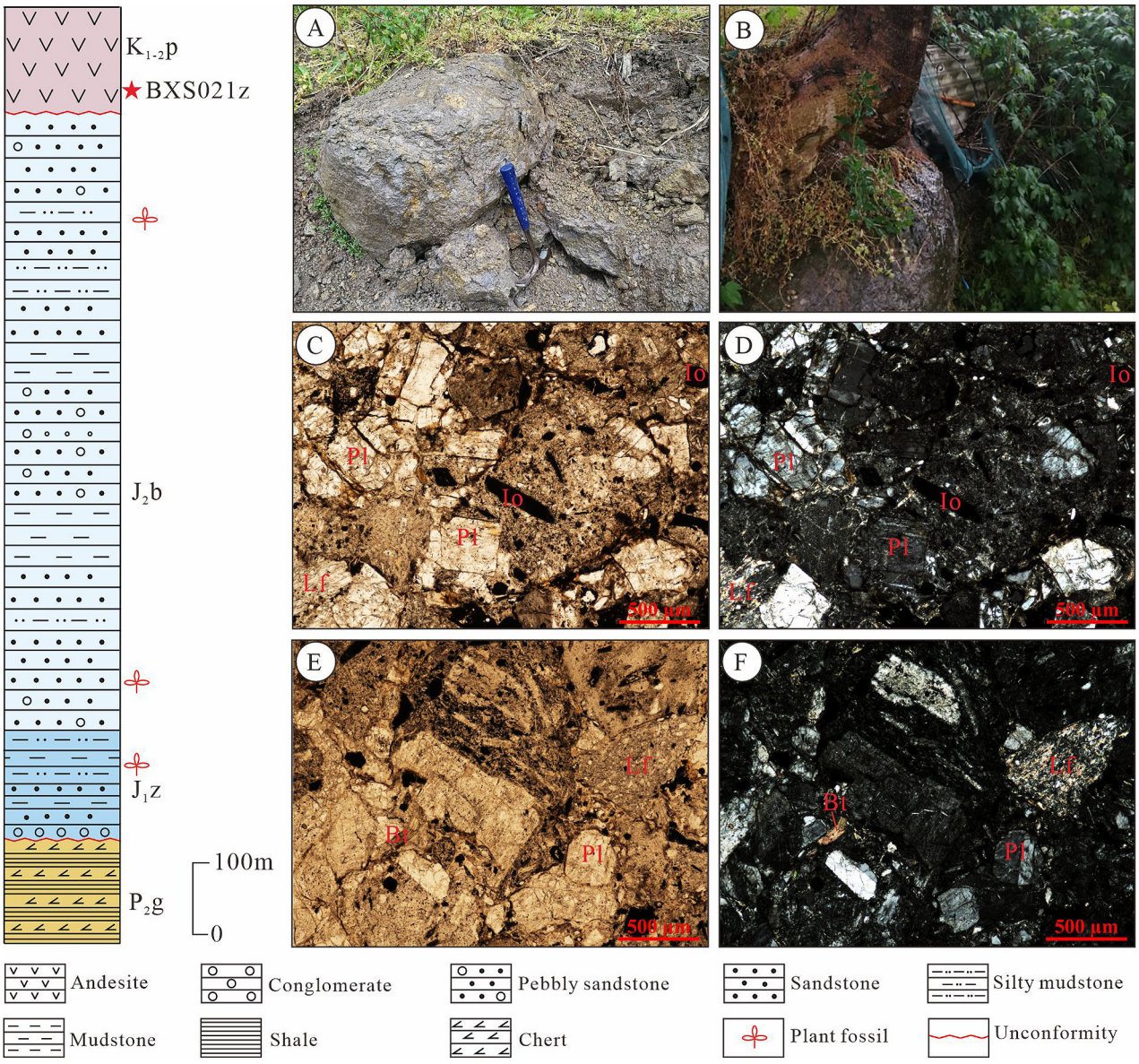

FIGURE 2. The stratigraphic column of the Beixiangshan Section, Nanjing. **A**, **B**, Filed photos. **C**–**F**, Photomicrographs for the sample BXS021z. (**C**, **E**, under the plane-polarized light; **D**, **F**, crossed nicols). Abbreviations: Pl, plagioclase; Io, Iron oxide; Lf, lithic fragment; P_2g, the Upper Permian Gufeng Formation; J_1z, the Lower Jurassic Nanxiangshan Formation; J_2b, the Middle Jurassic Beixiangshan Formation; $K_{1-2}P$, the Early-Late Cretaceous Pukou Formation.

grinding the fresh portions into powders of 200 mesh using an agate mortar for elemental analyses. The major elements were analysed using inductively coupled plasma optical emission spectrometer (ICP-OES) with an Agilent Technologies 710, and the trace elements were analysed by inductively coupled plasma mass spectrometry (ICP-MS) with an Agilent Technologies 7700x. Both analyses were conducted at the Public Technical Service Center of Nanjing Institute of Geology and Palaeontology, Chinese Academy of Sciences.

Results

Zircon U-Pb ages

The zircon grains extracted from the andesite display characteristics of being colourless and euhedra, typically measuring 50–200 μm in length, with length-to-width ratios spanning from 1:1 to 4:1. Most of the grains exhibit well-developed oscillatory zoning in CL images (Fig. 3). The analyses of the zircons yield a wide range of Th (144–1104 ppm) and U (149–506 ppm) concentrations, with Th-U ratios range from 0.6 to 2.4, indicative of

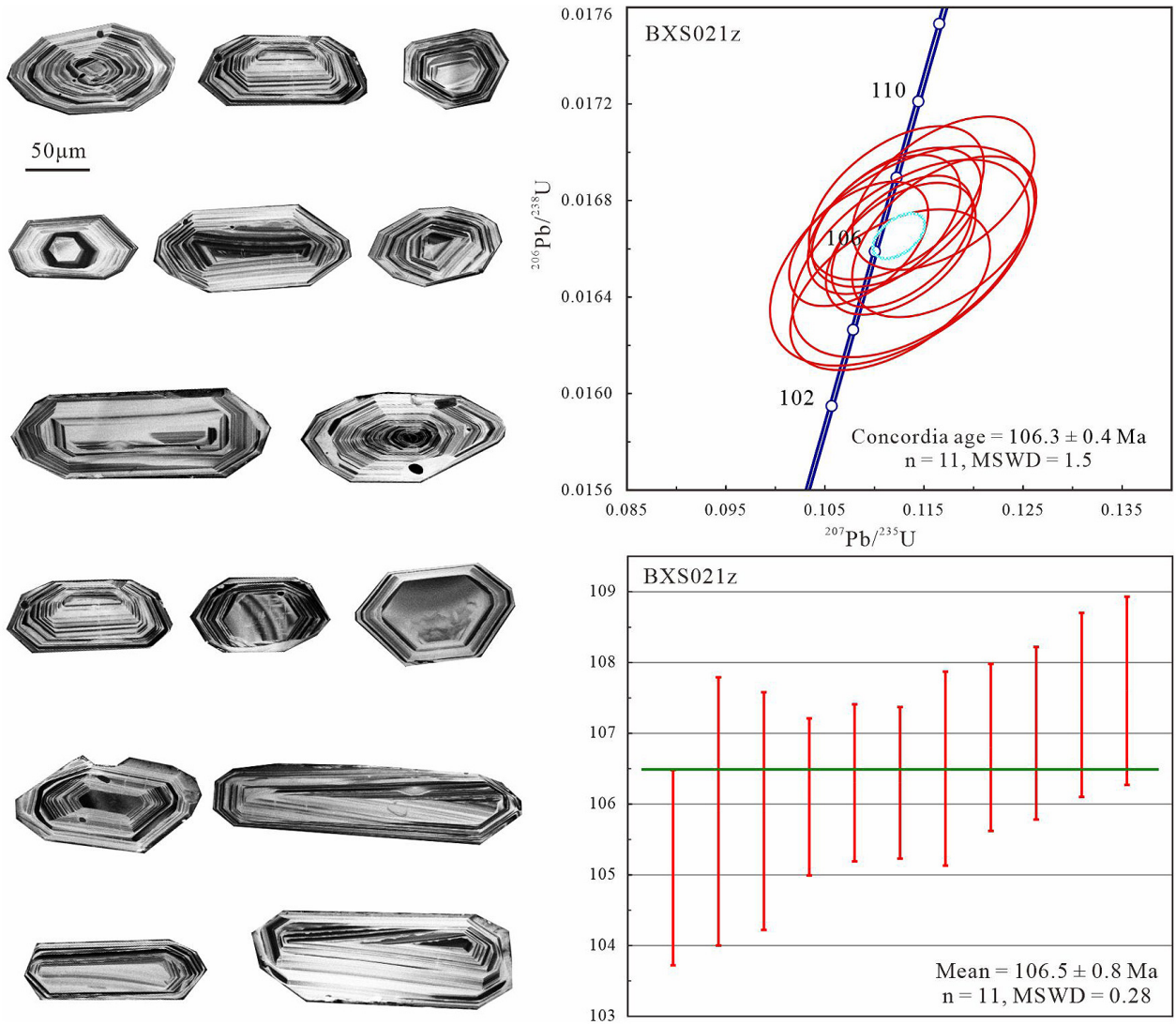

FIGURE 3. Cathodoluminescence (CL) images of representative zircons and zircon U-Pb concordant and weighted mean age plots for the volcanic rocks from the Beixiangshan Section, Nanjing, China. The error is 1 σ.

an igneous origin. Scattered data or those with lower concord (typically < 90%) were excluded when plotting the concordia and weighted mean age plots.

Thirty-one grains were analszed. Nine analyses were excluded due to low concordance, and eight analyses were rejected for their scattered distribution. Another three analyses yielded older ages of 221 ± 2 Ma, 159 ± 1 Ma and 128 ± 3 Ma, respectively, which were regarded as inherited ages. The remaining eleven concordant analyses yielded a concordia age of 106.3 ± 0.4 Ma and a weighted mean age of 106.5 ± 0.8 Ma.

Geochemical characteristics

Six samples were analysed on the major and trace element compositions, and the data are shown in Table 2 and Fig. 4. The samples predominantly fall within the andesite and dacite fields on the total alkali-silica (TAS) (Fig. 4A), as well as the Zr/Ti*0.0001 vs Nb/Y diagrams (Fig. 4B). In the K_2O vs SiO_2 diagram, the samples are plotted into the medium- to high-K cal-alkaline fields (Fig. 4C). These rocks have low K_2O (1.3–2.3 wt.%) and Na_2O (0.6–1.2 wt.%) contents, with K_2O/Na_2O ratios varying from 1.5 to 2.8 (Fig. 4D, Table 2). All samples are characterized by low TiO_2 content (0.9–1.1 wt.%), low Mg# value (27–37) and moderate Al_2O_3 content (12.8–16.1 wt.%).

All the samples show enrichment of light rare earth elements (LREEs) and depletion of heavy rare earth elements (HREEs) in the chondrite-normalized REE diagram, with a $(La/Yb)_N$ ranging from 16.6 to 21.5 (average is 19.1, Fig. 5A). Some rocks have slightly negative Eu anomalies (Eu/Eu* = 0.88–1.03), with a mean value of 0.96. In the primitive mantle-normalized diagram (Fig. 5B), the samples exhibit typical arc-like distribution patterns, showing enrichment in LREEs and

TABLE 2. Major and trace element analytical data for the volcanic rocks in the Beixiangshan area, Nanjing City, China.

Sample	BXS-01	BXS-02	BXS-03	BXS-04	BXS-05	BXS-06
Major elements (ppm)						
K	13905.51	19106.00	17933.01	16356.56	10375.00	11219.45
Na	4511.78	6515.25	6516.00	8609.42	6280.14	4421.42
Ca	67439.75	86221.99	64066.29	77351.70	84662.14	71360.11
Al	66970.64	84641.55	80286.86	69728.28	71583.70	70178.52
Fe	47265.92	53225.83	54105.46	41092.81	45610.34	47615.99
Mg	8248.66	11470.21	10870.23	8106.48	11271.99	11579.17
P	1875.35	1992.58	2044.79	1110.07	1159.08	1258.77
Trace elements (ppm)						
Li	27.44	26.60	27.19	14.26	27.15	28.41
Be	1.34	1.31	1.39	0.65	1.18	1.19
Sc	23.43	27.26	24.99	18.61	19.76	21.53
Ti	5998.07	5933.85	6655.85	5817.04	4963.11	5346.57
V	253.25	268.23	285.58	210.21	199.91	211.38
Cr	67.04	80.64	88.62	25.89	39.55	42.44
Mn	1122.25	1228.03	919.49	1148.63	1259.03	1146.67
Co	18.86	18.51	17.71	12.27	18.48	19.19
Ni	14.41	15.31	15.52	7.29	13.20	12.99
Cu	60.71	65.77	61.81	31.29	49.27	43.44
Zn	45.08	52.98	52.99	60.15	56.50	56.90
Ga	15.95	17.04	17.67	16.55	15.88	15.90
Ge	4.77	5.07	5.26	3.94	4.43	4.36
Rb	29.51	60.61	45.98	61.37	27.73	33.58
Sr	200.45	294.22	263.63	227.41	187.16	171.77
Y	22.70	25.61	24.87	22.23	20.84	17.86
Zr	156.62	161.55	168.44	170.93	135.09	179.92
Nb	6.73	6.86	7.20	6.00	5.39	5.50
Mo	1.23	0.97	1.01	0.32	0.78	0.92
Cd	0.17	0.18	0.17	0.45	0.16	0.19
Sn	0.87	0.81	0.94	0.82	0.83	0.77
Cs	4.60	4.44	4.20	2.99	3.89	5.61
Ba	586.93	824.54	789.21	197.68	346.59	449.43
La	44.04	52.68	49.47	40.40	39.89	32.94
Ce	62.89	79.52	72.12	49.22	51.73	51.30
Pr	9.04	10.33	10.09	7.08	7.19	6.44
Nd	36.24	41.05	40.20	27.77	28.15	25.61
Sm	6.83	7.66	7.49	5.16	5.20	4.80
Eu	1.88	2.14	2.05	1.65	1.91	1.44
Gd	6.06	6.95	6.77	4.66	4.71	4.30
Tb	0.74	0.82	0.81	0.60	0.59	0.54
Dy	4.01	4.43	4.35	3.45	3.28	3.03
Ho	0.76	0.82	0.82	0.68	0.64	0.59
Er	1.92	2.07	2.10	1.82	1.67	1.54
Tm	0.26	0.28	0.28	0.25	0.23	0.22
Yb	1.67	1.76	1.79	1.63	1.46	1.42
Lu	0.25	0.26	0.27	0.24	0.22	0.21
Hf	3.70	3.77	4.00	4.02	3.17	4.16
Ta	0.32	0.31	0.34	0.29	0.27	0.27
W	0.59	0.63	0.59	0.32	0.50	0.54
Pb	8.15	8.33	8.96	6.70	8.59	9.11
Bi	0.06	0.06	0.06	0.05	0.32	0.28
Th	6.96	7.92	7.72	5.58	4.75	4.86
U	0.66	0.96	0.81	0.78	0.72	0.80

.....continued on the next page

TABLE 2 (Continued)

Sample	BXS-01	BXS-02	BXS-03	BXS-04	BXS-05	BXS-06
Calculation results						
SiO_2 (wt.%)	65.348	57.083	60.912	63.820	62.455	64.391
K_2O (wt.%)	1.691	2.324	2.182	1.988	1.260	1.363
K_2O+Na_2O (wt.%)	2.304	3.211	3.069	3.158	2.113	1.964
MgO (wt.%)	1.387	1.930	1.829	1.362	1.893	1.945
FeOT (wt.%)	6.565	7.317	7.493	5.683	6.376	6.544
Mg#	27.357	31.978	30.324	29.939	34.606	34.638
Nb/U	10.19	7.15	8.92	7.71	7.44	6.89
Ce/Pb	7.72	9.54	8.05	7.34	6.02	5.63
Ba/Th	84.31	104.14	102.22	35.44	73.04	92.47
Sr/Y	8.83	11.49	10.60	10.23	8.98	9.62
Eu/Eu*	0.88	0.88	0.86	1.01	1.16	0.95
$(La/Sm)_N$	4.16	4.16	4.16	4.16	4.16	4.16
$(Dy/Yb)_N$	1.60	1.69	1.63	1.42	1.51	1.43
$(La/Yb)_N$	18.88	21.52	19.88	17.79	19.65	16.63
$(La/Nb)_N$	6.79	7.97	7.13	6.99	7.68	6.22

$Mg^{\#}=100*(MgO/40.3044)/(MgO/40.3044+FeO_T/71.844)$; $Eu/Eu^*=2Eu_N/(Sm_N+Gd_N)$

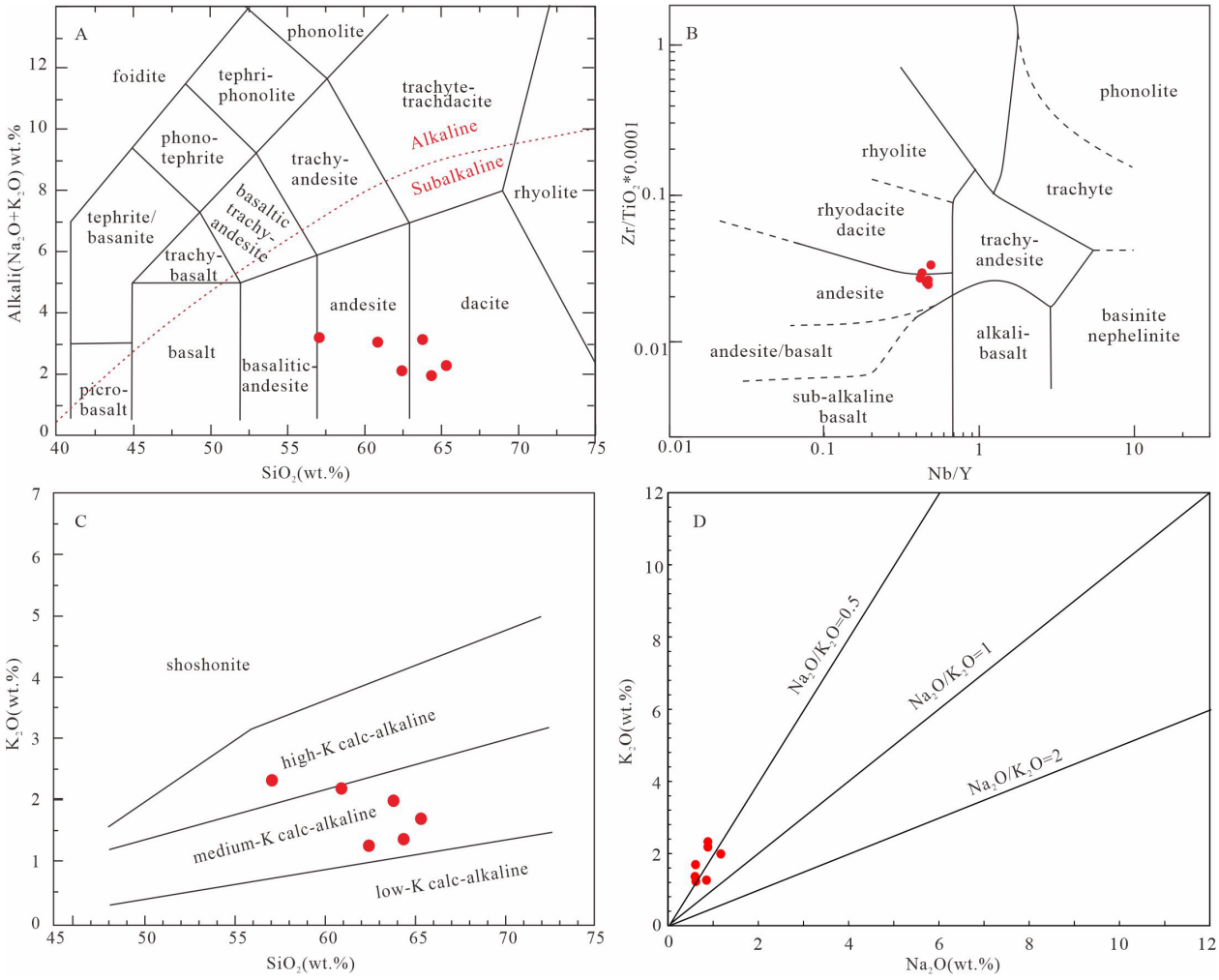

FIGURE 4. A series of classification diagrams for the igneous rocks in the Beixiangshan area, LYBR, South China. **A**, Total alkali vs. SiO_2 (TAS) diagram (after Le Bas *et al*., 1986). **B**, Zr/Ti*0.0001 vs. Nb/Y diagram (after Winchester & Floyd, 1977). **C**, K_2O vs. SiO_2 diagram (after Le Maitre *et al*., 1989). **D**, K_2O vs. Na_2O diagram (Peccerillo & Taylor, 1976).

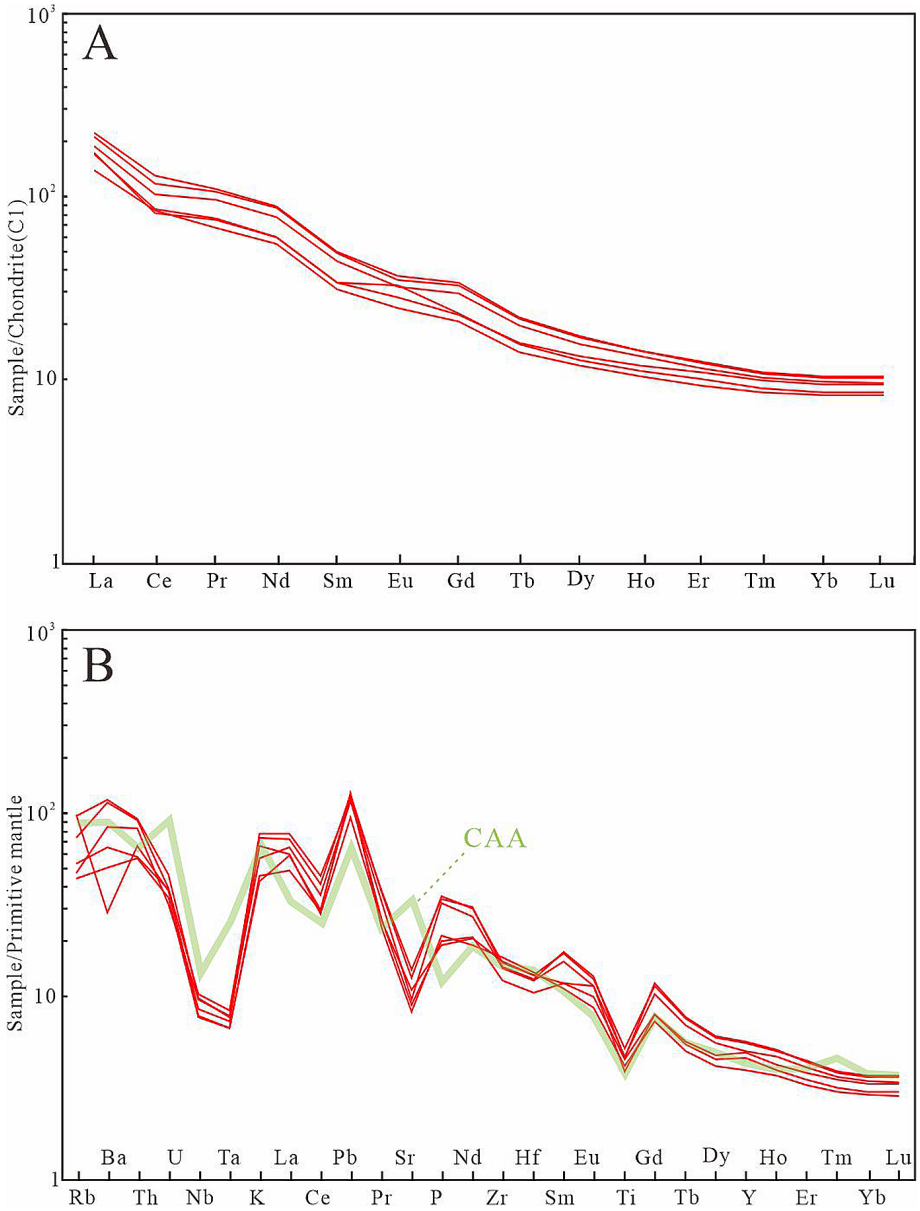

FIGURE 5. The normalized diagrams for the volcanic rocks of Beixiangshan. in the Ningzhen area, LYRB. A, Chondrite-normalized rare earth element patterns. B, Primitive mantle-normalized spider diagram. The normalization values of chondrite and primitive mantle are from (Sun & Mc Donough, 1989). Data of continental arc andesite (CAA) are from Zheng, 2012.

large ion lithophile elements (LILEs), such as Rb, Th, U, and Pb, and depletion in the high field-strength elements (HFSEs), including Nb, Ta, P, and Ti.

Discussion

Age of the volcanic rocks

The volcanic rocks in the Beixiangshan area were previously assigned to the Jurassic Xiangshan Group or Longwangshan Formation. However, dating evidence now suggests that these rocks actually formed during the late Early Cretaceous period (*ca.* 106 Ma, in the Albian stage), marking the final phase of the Yanshannian magmatic activity in the LYRB.

The late Albian to Cenomanian Pukou Formation nearby consists of a suit of conglomerates at the base and grey to purple volcanic rocks and their related pyroclastic deposits in the lower part (Song, 1986; JBGMR, 1997). This unit is the highest Mesozoic layer containing volcanic materials in this region, and its maximum depositional age approximate to the age (106 Ma) indicated by our study. The base of the Pukou Formation in this area was considered as piedmont deposits, consisting of andesitic and trachyandesitic compositions, resembling those observed in our study area. The depocenter for these

deposits is located in Puzhen, Nanjing, in close proximity to our research site. Considering their petrological and spatiotemporal affinities, it is possible that the volcanic rocks in the Beixiangshan area are part of the lower part of the Pukou Formation.

Tectonic setting

As shown in Fig. 5, the patterns of these rocks closely resemble those of normal subduction-relational, arc-type magma. Usually, the calc-alkaline andesite lavas are found almost exclusively in arcs (Gill, 1981), and their arc-like geochemical signatures are inherited from the mantle wedge that was metasomatized by the liquid phase produced by dehydration and melting of the subducting oceanic crust (Chen *et al*., 2020).

The Th-Hf-Ta diagram is successful in distinguishing the destructive plat-margin lavas from those erupted in other tectonic environments (Wood, 1980). All the samples are plotted within the "calc-alkaline basalt" field (Fig. 6A), indicating an arc-relation setting. Furthermore, La/Nb and Ba/Nb ratios in these rocks exceed those of OIB, primitive mantle, N-MORB, and average continental crust (Fig. 6B), but are similar to those of arc volcanic rocks. The Sr/Y *vs*. Y and $(La/Yb)_N$ *vs*. Yb diagrams(Fig. 6C, D) are typically utilized for the discrimination of adakitic and arc-related rocks (Defant *et al*., 2002, Zhao *et al*., 2009). The samples from Beixiangshan are plotted into the normal arc-related field (Fig. 6C) and their transition region (Fig. 6D).

There are several contemporaneous intrusions nearby, including the Anjishan pluton, which is located about 10 km away and intruded during the period of 108-106 Ma (Zeng *et al*., 2013; Liu *et al*., 2014; Wang X. *et al*., 2014). Despite intruding synchronously with the eruption of the volcanic rocks, they exhibit distinct geochemical features. Rocks from the intrusions are characterized by High Na_2O, Ba, and Sr contents, enrichment of LREEs, and depletion of HREEs and HFSEs (Xu *et al*., 2002; Xue, 2019). The rocks usually fall within the "adakitic rock" fields in the Sr/Y *vs*. Y and $(La/Yb)_N$ *vs*. Yb diagrams (Figs 6A, B) due to their high Sr, Low Y and Yb contents. The low Y contents of the adakitic rocks are attributed to the presence of residual garnet in the source region (Defant *et al*., 2002), which is generally related to a thicken LCC (Xu *et al*., 2002; Wang X. *et al*., 2014; Wang F. *et al*., 2014). Considering their temporal and spatial affinity, the volcanic rocks and the intrusions are likely formed in similar settings and may share genetic relationships. While they show "arc-like" and "adakite-like" geochemical signatures, respectively, indicating the complexity of the deep lithospheric processes.

Although the petrogenesis and tectonic setting of the Cretaceous magmatic activities in the LYRB are still a topic of much debate among scholars (*e.g*., Xu *et al*., 2002; Li e*t al*., 2013; Chen *et al*., 2014, 2020; Yan *et al*., 2015, 2021). However, it is widely acknowledged that these rocks were generally formed in an extensional environment, with their spatial and temporal distribution being controlled by the subduction and rollback of the Paleo-Pacific. There was a period of magmatic quiescence (*ca*. 117–109 Ma) in all of the SE China coast area, which was considered as a response to a weak compressional event (*e.g*., Charvet *et al*., 1994; Li *et al*., 2015; Zhu *et al*., 2018). Considering that, the last stage of magmatic activity (109–100 Ma) may be formed during the transition phase from compression to extension.

Tectonic implications

The westward subduction of the Paleo-Pacific has led to significant amounts of magmatic activities along the southeastern coast of China (*e.g*., Li, 2000; Zhou & Li, 2000; Liu *et al*., 2020). Although, there are differences in rock type of the Early Cretaceous igneous rocks between the SE coastal area and the LYRB, they exhibit similar temporal and spatial patterns of magmatism, including: 1) an eastward younging trend of the magmatism (Zhou & Li, 2000; Liu *et al*., 2014; Sun *et al*., 2017; Liu e*t al*., 2020); 2) a period of magmatic quiescence that separates two episodes of extension-related magmatism (Charvet *et al*., 1994). The former is believed to be the result of the rollback of the Paleo-Pacific slab (Zhou & Li, 2000), and the latter is considered as a response to the change in the subduction direction of the Paleo-Pacific plate (Sun *et al*., 2007; Tang *et al*., 2013; Tan *et al*., 2023).

The periods of magmatic quiescence in the coast area and LYRB were suggested as occurring between 117–105 Ma (Li *et al*., 2014a; Li *et al*., 2015) and 122–109 Ma (Sun *et al*., 2013; Liu *et al*., 2014; Xue, 2019), respectively.

This tectonic event was also recorded by some large faults parallel to the subduction zone, such as the activity of NE-trending Changle-Nan'ao ductile shear zone during 120–100 Ma (dated by muscovite $^{40}Ar/^{39}Ar$, Wang & Lu, 2000) and the Early Cretaceous sinistral faulting event postdating 124 Ma. Therefore, the timing of this weak compressional event, resulting from changes in the convergent direction of the Paleo-Pacific, is constrained to about 120–109 Ma.

This event also led to a regional angular unconformity between the upper Cretaceous coarse-grained clastic rocks and the underlying lower Cretaceous volcanic rocks in the coastal areas of Zhejiang and Fujian (Lapierre *et al*., 1997; Wang *et al*., 2013). A suite of 105–95 Ma igneous rocks that generally unconformably overlies older strata includes the Yongkang and/or Qujiang groups in the Zhejiang Province, the Shimaoshan Group in the Fujian and eastern Guangzhou Provinces (Guo *et al*., 2012; Cao *et al*., 2021), and the Liuluocun Formation in the Hainan Province (HBGMR, 1997). The angular unconformity

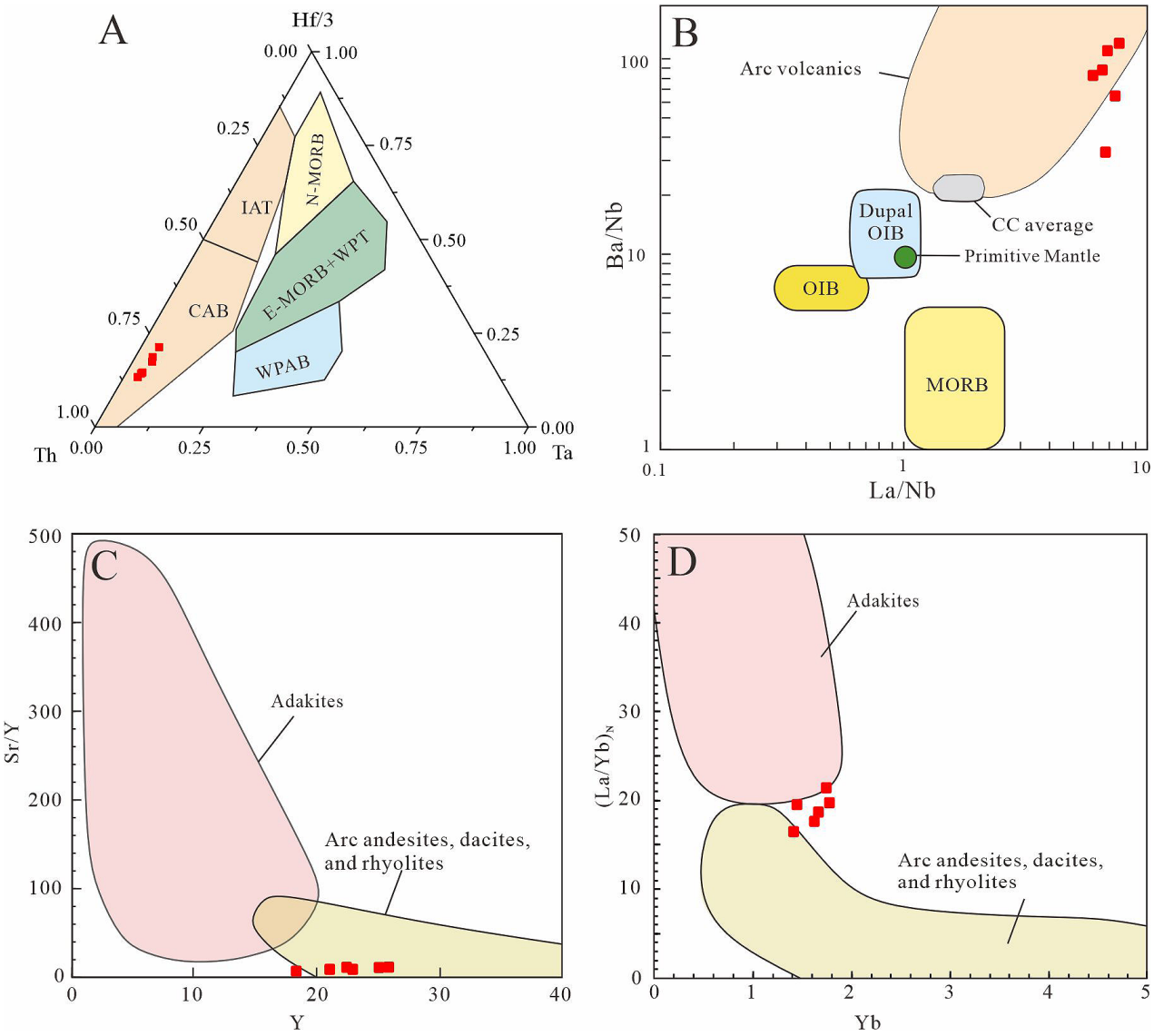

FIGURE 6. Variations discrimination diagrams for the volcanic rocks in the Beixiangshan area. **A**, Th-Hf-Ta. **B**, Ba/Nb *vs*. La/Nb. **C**, Sr/Y (a) *vs*. Y. **D**, $(La/Yb)_N$ *vs*. Yb. The compositions of different end-members in **A** and **B** are after Wilson, 2001 and Wood, 1980, respectively. The range of adakite and arc magmatic rocks is after Defant & Drummond, 1990. Abbreviation: MORB, mid-ocean ridge basalt; N-MORB, normal mid-oceanic ridged basalt; E-MORB, enriched mid-oceanic ridged basalt; WPT, within-plate tholeiitic lavas; WPAB, within-plate alkaline basalt; IAT, island arc tholeiitic lavas; CAB, calc-alkaline basalt; OIB, oceanic island basalt; CC, continental crust.

beneath these units is widely comparable, perhaps representing the episode C of Yanshanian tectonic events (Dong *et al*., 2015; Zhu *et al*., 2018).

The volcanic rocks in the Beixiangshan area erupted subsequent to a compressional tectonic event, indicating their formation during a transition phase from compressional to extensional environments resulting from direction changes of the plate convergence. In addition, these volcanic rocks provide a minimum age of *ca.* 106 Ma for the angular unconformity in the LYRB.

Conclusion

The newly identified volcanic rocks in the Beixiangshan area erupted at *ca.* 106 Ma, contradicting previous assumptions that they belonged to either the Longwangshan Formation or the Xiangshan Group. These volcanic rocks represent the final episode of the Yanshannian magmatic activities in the LYRB.

This suit of volcanic rocks is characterized by arc-like geochemical features, differing from the intrusions

in the Ningzhen area. They formed in a transition from a compressional to an extensional environment, a result of the change in plate convergence direction.

The regional angular unconformity beneath the Pukou Formation is interpreted as representing the Episode C of Yanshanian tectonic events. The volcanic rocks in the Beixiangshan provide a minimum age constraint on the angular unconformity, dating it to 106 Ma.

Acknowledgments

We thank two anonymous reviewers for their valuable comments on an earlier version of this paper. This work was supported by the National Natural Science Foundation of China (41925008).

References

Cao, X.Z., Flament N., Li, S.Z. & Müller, R.D. (2021) Spatio-temporal evolution and dynamic origin of Jurassic-Cretaceous magmatism in the South China Block. *Earth-Science Reviews*, 217, 103605. https://doi.org/10.1016/j.earscirev.2021.103605

Charvet, J., Lapierre, H. & Yu, Y.W. (1994) Geodynamic significance of the Mesozoic volcanism of southeastern China. *Journal of Southeast Asian Earth Sciences*, 9 (4), 387–396. https://doi.org/10.1016/0743-9547(94)90050-7

Chen, J.F., Foland K.A., Xing, F., Xu, X & Zhou, T.X. (1991) Magmatism along the southeast margin of the Yangtze block: Precambrian collision of the Yangtze and Cathysia blocks of China. *Geology*, 19, 815–818. https://doi.org/10.1130/0091-7613(1991)019<0815:MATSMO>2.3.CO;2

Chen, L., Zhao, Z.F. & Zheng, Y.F. (2014) Origin of andesitic rocks: geochemical constraints from Mesozoic volcanics in the Luzong basin, South China. *Lithos*, 190, 220–239. https://doi.org/10.1016/j.lithos.2013.12.011

Chen, L., Zheng, Y.F. & Zhao, Z.F. (2016) Geochemical constraints on the origin of late Mesozoic andesites from the Ningwu basin in the Middle-Lower Yangtze Valley, South China. *Lithos*, (254–255), 94–117. https://doi.org/10.1016/j.lithos.2016.03.012

Chen, L., Zheng, Y.F. & Zhao, Z.F. (2020) Origin of arc-like magmatism at fossil convergent boundaries: Geochemical insights from Mesozoic igneous rocks in the Middle to Lower Yangtze Valley, South China. *Earth-Science Reviews*, 211, 103416. https://doi.org/10.1016/j.earscirev.2020.103416

Defant, M.J., Xu, J.F., Kepezhinskas, P., Wang, Q., Zhang, Q. & Xiao, L. (2002) Adakites: some variations on a theme. *Acta Petrological Sinica*, 18, 129–142.

Dong, S.W, Zhang, Y.Q., Zhang, F.Q., Cui, J.J., Chen, X.H., Zhang, S.H., Miao, L.C., Li, J.H., Shi, W., Li., Z.H., Huang, S.Q. & Li, H.L. (2015) Late Jurassic-Early Cretaceous continental convergence and intracontinental orogenesis in East Asia: A synthesis of the Yanshan Revolution. *Journal of Asian Earth Sciences*, 114, 750–770. https://doi.org/10.1016/j.jseaes.2015.08.011

Geological Bureau of Anhui Province (GBAP) (1986) *Regional geological survey report (Nanjing part)*. [In Chinese]

Gill, J.B. (1981) *Orogenic andesites and plate tectonics*. Springer-Verlag, New York, pp. 390. https://doi.org/10.1007/978-3-642-68012-0

Guo, F., Fan, W., Li, C., Zhao, L., Li, H. & Yang, J. (2012) Multi-stage crust-mantle interaction in SE China: temporal, thermal and compositional constraints from the Mesozoic felsic volcanic rocks in eastern Guangdong—Fujian provinces. *Lithos*, 50, 62–84. https://doi.org/10.1016/j.lithos.2011.12.009

Guo, F., Li, H.X., Fan, W.M., Li, J.Y., Zhao, L., Huang, M.W. & Xu, W.L. (2015) Early Jurassic subduction of the Paleo-Pacific Ocean in NE China: petrologic and geochemical evidence from the Tumen mafic intrusive complex. *Lithos*, 224–225, 46–60. https://doi.org/10.1016/j.lithos.2015.02.014

Hainan Bureau of Geology and Mineral Resources (HBGMR) (1997) *Strata of the Hainan Province*. China University of Geosciences Press, Wuhan, pp. 128. [In Chinese]

Huang, P. (2000) Discovery of Middle Jurassic palynological assemblage from Beixiangshan of Nanjing. *Acta Micropalaeontologica Sinica*, 17(4), 457–469. [In Chinese with English abstract]

Jiangsu Bureau of Geology and Mineral Resources (JBGMR) (1997) Strata of the Jiangsu Province. China University of Geosciences Press, Wuhan, pp. 288. [In Chinese]

Ju, K.X. (1987) Subdivision of the Lower-Middle Jurassic strata in south Jiangsu. Bull of Nanjing Institute of Geology and Mineral Resources, 8 (4), 33–44. [In Chinese]

Lapierre, H, Jahn, B.M, Charvet, J. & Yu, Y.W. (1997) Mesozoic felsic arc magmatism and continental olivine tholeiites in Zhejiang Province and their relationship with the tectonic activity in southeastern China. *Tectonophysics*, 274 (4), 321–338. https://doi.org/10.1016/S0040-1951(97)00009-7

Le Bas, M.J., Le Maitre, R.W., Streckheisen, A. & Zanettin, B. (1986) A chemical classification of volcanic rocks based on the total alkali-silica diagram. *Journal of Petrology*, 27, 745–750. https://doi.org/10.1093/petrology/27.3.745

Le Maitre, R.W., Bateman, P., Dudek, A., Keller, J., Lameyre, J., Le Bas, M.J., Sabine, P.A., Schmid, R., Sorensen, H., Streckeisen, A., Woolley, A.R. & Zanettin, B. (1989) A classification of igneous rocks and glossary of terms: Recommendations of the International Union of Geological Sciences Subcommission

on the Systematics of Igneous Rocks. Blackwell Scientific, Oxford, pp.193.

Li, J.H., Ma, Z.L., Zhang, Y.Q., Dong, S.W., Li, Y., Lu, M.A. & Tan, J.Q. (2014a) Tectonic evolution of Cretaceous extensional basins in Zhejiang Province, eastern South China: structural and geochronological constraints. *International Geology Review*, 56 (13), 1602–1629. https://doi.org/10.1080/00206814.2014.951978

Li J.H., Zhang Y.Q., Dong, S.W. & Johnston, S.T. (2014b) Cretaceous tectonic evolution of South China: a preliminary synthesis. *Earth-Science Reviews*, 134, 98–136. https://doi.org/10.1016/j.earscirev.2014.03.008

Li, X.H. (2000) Cretaceous magmatism and lithospheric extension in Southeast China. *Journal of Asian Earth Sciences*, 18 (3), 293–305. https://doi.org/10.1016/S1367-9120(99)00060-7

Li, Y, Ma CQ., Xing, G.F. & Zhou, H.W. (2015) The Early Cretaceous evolution of SE China: insights from the Changle-Nan'ao Metamorphic Belt. *Lithos*, 230, 94–104. https://doi.org/10.1016/j.lithos.2015.05.014

Ling, M.X., Wang, F.Y., Ding, X., Hu, Y. H., Zhou, J.B., Zartman, R.E., Yang, X.Y. & Sun, W.D. (2009) Cretaceous ridge subduction along the Lower Yangtze River Belt, eastern China. *Economic Geology*, 104, 303–321. https://doi.org/10.2113/gsecongeo.104.2.303

Liu, J.M., Yan, J., Li, Q.Z. & Liu, X.Q. (2014) Zircon La-ICPMS dating of the Anjishan Pluton in Nanjing-Zhenjiang Area and its significance. *Geological Review*, 60 (1), 190–200. [In Chinese with English abstract]

Liu, J.X., Wang, S., Wang, X.L., Du, D.H, Xing, G.F., Fu, J.M., Chen, X. & Sun, Z.M. (2020) Refining the spatio-temporal distributions of Mesozoic granitoids and volcanic rocks in SE China. *Journal of Asian Earth Sciences*, 201, 104503. https://doi.org/10.1016/j.jseaes.2020.104503

Ludwig, K.R. (2003) *User's manual for Isoplot 3.0. A geochronological toolkit for Microsoft Excel*. Berkeley Geochronology Centre: Berkeley, California, Special Publication, 4a, 1–70.

Mao, J.W., Xie, G.Q., Duan, C., Pirajno, F., Ishiyama, D., & Chen, Y.C. (2011) A tectono-genetic model for porphyry-skarn-stratabound Cu-Au-Mo-Fe and magnetite-apatite deposits along the Middle-Lower Yangtze River Valley, Eastern China. *Ore Geology Reviews*, 43 (1), 294–314. https://doi.org/10.1016/j.oregeorev.2011.07.010

Meng, Q.R. & Zhang, G.W. (1999) Timing of collision of the North and South China blocks: controversy and reconciliation. *Geology*, 27 (2), 123–126. https://doi.org/10.1130/0091-7613(1999)027<0123:TOCOTN>2.3.CO;2

Peccerillo, Angelo &Taylor, S. R. (1976) Geochemistry of Eocene calc-alkaline volcanic rocks from the Kastamonu area, northern Turkey. *Contributions to mineralogy and petrology*, 58, 63–61. https://doi.org/10.1007/BF00384745

Song, Z.C. (1986) A review of the study of early Cretaceous angiosperm pollen in China. *Acta Micropalaeontologica Sinica*, 3(4), 373–380. [In Chinese with English abstract]

Sun, S.S. & McDonough, W.F. (1989) Chemical and isotopic systematics of oceanic basalts: implications for mantle composition and processes. *Geological Society, London, Special Publications*, 42, 313–345. https://doi.org/10.1144/GSL.SP.1989.042.01.19

Sun, W.D., Ding, X., Hu, Y.H, & Li, X.H. (2007) The golden transformation of the Cretaceous plate subduction in the west Pacific. *Earth and Planetary Science Letters*, 262 (3), 533–542. https://doi.org/10.1016/j.epsl.2007.08.021

Sun, W.A., Yuan, F., Jowitt, S.M., Zhou, T.F., Hollings P, Liu, G.X., & Li, X.F. (2017) Geochronology and geochemistry of the Fe ore-bearing Zhonggu intrusions of the Ningwu Basin: implications for tectonic setting and contemporaneous Cu-Au mineralization in the Middle-Lower Yangzte Metallogenic Belt. *Ore Geology Reviews*, 84, 246–272. https://doi.org/10.1016/j.oregeorev.2017.01.007

Sun, Y., Ma, C.Q. & Liu, B. (2013) The latest Yanshanian magmatic and metallogenic events in the middle-lower Yangtze River belt: evidence from the Ningzhen region. *Chinese Science Bulletin*, 58 (34), 4308–4318. https://doi.org/10.1007/s11434-013-6015-8

Sun, Y., Ma, C.Q. & Liu, B. (2021) Important role of magma mixing in generating the Late Cretaceous Shima intrusion along the Middle-Lower Yangtze River belt: evidence from petrology, geochemistry, and zircon U-Pb-Hf isotopes. *Lithos*, 390–391, 106143. https://doi.org/10.1016/j.lithos.2021.106143

Tan, Y.L., Wang, Z.X., Li, C.L., Yan, X.L. & Peng, N. (2023) Mesozoic tectonic regime transformation in Fujian Province (Southeast China): evidence from palaeostress field restoration and lithofacies paleogeography evolution. *Geological Journal*, 59 (2), 701–731. https://doi.org/10.1002/gj.4888

Tang, Y.J., Zhang, H.F., Ying, J.F., Su, B.X., Li, X. H. & Santosh, M. (2013) Rapid eruption of the Ningwu volcanics in eastern China: response to Cretaceous subduction of the Pacific plate. *Geochemistry, Geophysics, Geosystems*, 14 (6), 1703–1721. https://doi.org/10.1002/ggge.20121

Wang, F.Y., Liu, S.A., Li, S.G., Akhtar, S. & He, Y.S. (2014) Zircon U-Pb ages, Hf-O isotopes and trace elements of Mesozoic high Sr/Y porphyries from Ningzhen, eastern China: Constraints on their petrogenesis, tectonic implications and Cu mineralization. *Lithos*, 200–201, 299–316. https://doi.org/10.1016/j.lithos.2014.05.004

Wang, X.L., Zeng, J.N., Ma, C.Q., Li, X.F., Wu, Y.F. & Lu, S.F. (2014) Zircon U-Pb dating of Yanshanian intrusive rocks in Ningzhen district, Jiangsu: the chronology evidence for a new stage of petrogenesis and metallogeny in the Middle and Lower Reaches of Yangtze River. *Earth Science Frontiers*, 21(6), 189–301. [In Chinese with English abstract] https://doi.org/10.13745/j.esf.2014.06.028

Wang, Y.J., Fan, W.M., Zhang, G.W., & Zhang. Y.H. (2013) Phanerozoic tectonics of the South China Block: key observations and controversies. *Gondwana Research*, 23 (4), 1273–1305. https://doi.org/10.1016/j.gr.2012.02.019

Wang, Z.H., & Lu, H. F. (2000) Ductile deformation and $^{40}Ar/^{39}Ar$ dating of the Changle-Nan'ao ductile shear zone, southeastern China. *Journal of Structural Geology*, 22 (5), 561–570. https://doi.org/10.1016/S0191-8141(99)00179-0

Wilson, M., (2001) Igneous petrogenesis. Chapman & Hall, London. 480 pp.

Winchester, J.A.& Floyd, P.A., (1977) Geochemical discrimination of different magma series and their differentiation products using immobile elements. *Chemical Geology*, 20, 325–343. https://doi.org/10.1016/0009-2541(77)90057-2

Wong, W.H. (1927) The Mesozoic orogenic movement in eastern China. *Geological Society of China Bulletin*, 8, 33–44. https://doi.org/10.1111/j.1755-6724.1929.mp8001004.x

Wood, D.A. (1980) The application of a Th-Hf-Ta diagram to problems of tectonomagmatic classification and to establishing the nature of crustal contamination of basaltic lava of the British Tertiary volcanic province. *Earth Planetary Science Letters*, 50, 11–30. https://doi.org/10.1016/0012-821X(80)90116-8

Xu, C.H., Zhang, Lu., Shi, H.S., Brix, M.R., Huhma, H., Chen, L.H. Zhang, M.Q. & Zhou, Z.Y. (2017) Tracing an Early Jurassic magmatic arc from South to East China Seas. *Tectonics*, 36 (3), 466–492. https://doi.org/10.1002/2016TC004446

Xu, J.F., Shinjo, R., Defant, M.J., Wang, Q. & Rapp, R.P. (2002) Origin of Mesozoic adakitic intrusive rocks in the Ningzhen area of east China: Partial melting of delaminated lower continental crust? *Geology*, 30 (12), 1111–1114. https://doi.org/10.1130/0091-7613(2002)030<1111:OOMAIR>2.0.CO;2

Xue, H.M. (2019) Late Mesozoic adakitic intrusive rocks in Ningzhen district, Lower Yangtze River Reaches: ages, geochemical and genesis. *Acta Geologica Sinica*, 93 (1), 147–169. [In Chinese with English abstract]

Yan, J., Liu, J.M., Li, Q.Z., Xing, G.F., Liu, X.Q, Xie, J.C., Chu, X.Q, & Chen. Z.H. (2015) In situ zircon Hf-O isotopic analyses of late Mesozoic magmatic rocks in the Lower Yangtze River Belt, central eastern China: implications for petrogenesis and geodynamic evolution. *Lithos*, 227, 57–76. https://doi.org/10.1016/j.lithos.2015.03.013

Yan, J., Liu, X.Q., Wang, S.N., Xie, J.C. & Liu J.M. (2021) Metallogenic type controlled by magma source and tectonic regime: geochemical comparisons of Mesozoic magmatism between the Middle-Lower Yangtze River Belt and the Dabie Orogen, eastern China. *Ore Geology Reviews*, 133, 104095. https://doi.org/10.1016/j.oregeorev.2021.104095

Yan, S.M., Zhou, J.S., Wang, Q.F., Guan, Y.M. & Yang, X.Q., (2001) The study of the Pukou Formation under the drills in northern Jiangsu. *Journal of Stratigraphy*, 25 (2), 144–149. [In Chinese with English abstract]

Zeng, J.N., Li, J.W., Chen, J.H. & Lu, J.P. (2013) SHRIMP zircon U-Pb dating of Anjishan intrusive rocks in Ningzhen district, Jiangsu, and its geological significance. *Earth Science*, 38 (1), 57–67. [In Chinese with English abstract]

Zhang, Q., Jian, P., Liu, D.Y., Wang, Y.L., Qian, Q., Wang, Y. & Xue, H.M. (2003) SHRIMP dating of volcanic rocks from Ningwu area and its geological implications. *Science in China (series D)*, 46 (8), 830–837. https://doi.org/10.1007/BF02879526

Zhao, Y. (1990) The Mesozoic orogenies and tectonic evolution of the Yanshan area. *Geological Review*, 36 (1), 1–13. [In Chinese with English abstract]

Zhao, Z.D., Mo, X.X., Dilek, Y., Niu, Y.L., Depaolo, D.J., Robinson, P., Zhu, D.C., Sun, C.G., Dong, G.C., Zhou, S., Luo, Z.H. & Hou, Z.Q. (2009) Geochemical and Sr-Nd-Pb-O isotopic compositions of the post-collisional ultrapotassic magmatism in SW Tibet: petrogenesis and implications for India intra-continental subduction beneath southern Tibet. *Lithos*, 113, 190–212. https://doi.org/10.1016/j.lithos.2009.02.004

Zheng Y. (2012) Metamorphic chemical geodynamics in continental subduction zones. *Chemical Geology*, 328, 5–48. https://doi.org/10.1016/j.chemgeo.2012.02.005

Zhou, T.F., Fan, Y., Yuan, F., Zhang, L.J., Qian, B., Ma, L. & Yang, X.F. (2011) Geochronology and significance of volcanic rocks in the Ning-Wu Basin of China. *Science China Earth Science*s, 54, 185–196. https://doi.org/10.1007/s11430-010-4150-5

Zhou, T.F., Wang, S.W., Fan, Y., Yuan, F., Zhang, D.Y. & White, N.C. (2015) A review of the intracontinental porphyry deposits in the Middle-Lower Yangtze River Valley metallogenic belt, Eastern China. *Ore Geology Reviews*, 65, 433–456. https://doi.org/10.1016/j.oregeorev.2014.10.002

Zhou, X.M. & Li, W.X. (2000) Origin of Late Mesozoic igneous rocks in Southeastern China: implications for lithosphere subduction and underplating of mafic magmas. *Tectonophysics*, 326 (3), 269–287. https://doi.org/10.1016/S0040-1951(00)00120-7

Zhu, G., Liu, C., Gu, C.C., Zhang, S., Li, Y.J., Su, N & Xiao, S.Y. (2018) Oceanic plate subduction history in the western Pacific Ocean: constraint from late Mesozoic evolution of the Tan-Lu Fault Zone. *Science China: Earth sciences*, 61 (4), 386–405. https://doi.org/10.1007/s11430-017-9136-4